



NURC

a NATO Research Centre
un Centre de Recherche de l'OTAN



PARTNERING
FOR MARITIME
INNOVATION

Reprint Series

NURC-PR-2012-008

Adaptive autonomous underwater vehicles for littoral surveillance The GLINT10 field trial results

Stephanie Kemna, Michael J. Hamilton, David T. Hughes,
Kevin D. LePage

May 2012

Originally published in:

Intelligent Service Robotics, Vol. 4, No. 4, pp. 245-258, 2011.

About NURC

Our vision

- To conduct maritime research and develop products in support of NATO's maritime operational and transformational requirements.
- To be the first port of call for NATO's maritime research needs through our own expertise, particularly in the undersea domain, and that of our many partners in research and technology.

One of three research and technology organisations in NATO, NURC conducts maritime research in support of NATO's operational and transformation requirements. Reporting to the Supreme Allied Commander, Transformation and under the guidance of the NATO Conference of National Armaments Directors and the NATO Military Committee, our focus is on the undersea domain and on solutions to maritime security problems.

The Scientific Committee of National Representatives, membership of which is open to all NATO nations, provides scientific guidance to NURC and the Supreme Allied Commander Transformation.

NURC is funded through NATO common funds and respond explicitly to NATO's common requirements. Our plans and operations are extensively and regularly reviewed by outside bodies including peer review of the science and technology, independent national expert oversight, review of proposed deliverables by military user authorities, and independent business process certification.



Copyright © NURC, 2011. NATO member nations have unlimited rights to use, modify, reproduce, release, perform, display or disclose these materials, and to authorize others to do so for government purposes. Any reproductions marked with this legend must also reproduce these markings. All other rights and uses except those permitted by copyright law are reserved by the copyright owner.

NOTE: The NURC Reprint series reprints papers and articles published by NURC authors in the open literature as an effort to widely disseminate NURC products. Users are encouraged to cite the original article where possible.

Adaptive autonomous underwater vehicles for littoral surveillance

The GLINT10 field trial results

Stephanie Kemna · Michael J. Hamilton ·
David T. Hughes · Kevin D. LePage

Received: 11 March 2011 / Accepted: 5 July 2011 / Published online: 27 July 2011
© The Author(s) 2011. This article is published with open access at Springerlink.com

Abstract Autonomous underwater vehicles (AUVs) have gained more interest in recent years for military as well as civilian applications. One potential application of AUVs is for the purpose of undersea surveillance. As research into undersea surveillance using AUVs progresses, issues arise as to how an AUV acquires, acts on, and shares information about the undersea battle space. These issues naturally touch on aspects of vehicle autonomy and underwater communications, and need to be resolved through a spiral development process that includes at sea experimentation. This paper presents a recent AUV implementation for active anti-submarine warfare tested at sea in the summer of 2010. On-board signal processing capabilities and an adaptive behavior are discussed in both a simulation and experimental context. The implications for underwater surveillance using AUVs are discussed.

Keywords Autonomous underwater vehicle · Autonomy · Behavior-based robotics · Target localization and tracking · On-board processing · Multi-static active sonar

1 Introduction

In recent years, the interest in unmanned systems for military applications has increased. Autonomous off-board sensor systems, such as autonomous underwater vehicles (AUVs), are attractive candidates to complement existing high-value assets such as frigates, helicopters, and submarines in a variety of undersea surveillance missions. Their advantages including reduced manning and risks for military personnel,

allowing them to carry out other tasks. Furthermore, they provide the potential for a networked system that is scalable, persistent, and cost-effective.

Thanks to recent advances in unmanned vehicle autonomy AUVs are becoming capable of operating without constant external control. This can reduce operator load, but is also necessary to overcome limitations imposed by the restricted underwater acoustic communications. However, most AUVs still lack many aspects to operate as fully autonomous agents in a dynamic environment. These are [35]:

- *situatedness*: the ability to acquire information about the environment solely through its sensors in interaction with the environment,
- *self-sufficiency*: the ability to sustain itself over extended periods of time,
- *adaptivity*: the ability to adjust itself to its environment, learn from it or evolve.

These three features are critical for an AUV to survive and successfully perform its missions in a dynamic environment. Self-sufficiency is mainly dependent on vehicle endurance, and thus battery capabilities and developments. This paper will describe work that aims to improve the AUV's situatedness and adaptivity for undersea surveillance applications.

1.1 Undersea surveillance

Undersea surveillance, as referred to in this paper, is the task of monitoring the underwater environment for undersea threats, in particular submarines. A specific scenario envisioned for unmanned underwater vehicles is the “hold at risk” scenario, i.e. monitoring all submarines that exit a port or transit a chokepoint [13].

S. Kemna (✉) · M. J. Hamilton · D. T. Hughes · K. D. LePage
NATO Undersea Research Centre, Viale San Bartolomeo 400,
19126 La Spezia, Italy
e-mail: kemna@nurc.nato.int

To be able to use AUVs in undersea surveillance, they need to be equipped with sensors to characterize the environment, such as sonar. There are two forms of sonar; passive and active [26]. In *passive sonar*, noise that is emitted by objects is detected by receiving *hydrophones* (underwater microphones). Passive sonar has the advantage of covertness, and has been used by submarines and surface ships to conduct anti-submarine warfare (ASW) operations [6]. However, modern submarines have become very quiet (emitting less noise), and regions of operational interest have shifted from deep and open waters where *ambient noise* tends to be low, to littoral areas with higher levels of ambient noise from for example ship traffic and biological activity. These factors have placed greater limits on the effectiveness of passive sonar, increasing the interest in active sonar [6].

In *active sonar*, a sonar source (transmitter) transmits a sonar signal (*ping*), which reflects from objects in the environment and is collected by a receiver. If the source and receiver are co-located, the geometry is *mono-static*. *Bi-static* geometries are those where one source and one receiver are spatially separated. In a *multi-static* geometry there are multiple sources and/or multiple receivers.

Active sonar transmissions “insonify” or “illuminate” submarines even if they emit little noise. While active sonar transmissions are generally not covert, the receivers can still be covert in a bi-static or multi-static scenario, and this is particularly compelling for the use of quiet AUVs with stealthy communications. By using active sonar, ambient noise issues are usually mitigated because the sound intensity levels of the echoes tend to be higher than typical ambient noise levels. Every signal has a *signal-to-noise ratio* (SNR), which is determined by comparing the level of the received transmission to the level of the received background noise. For constant noise levels, the higher the initial sound intensity, the higher the SNR, and the less obtrusive the background noise is. However, active sonar suffers from *reverberation*, primarily in littoral areas. Reverberation is the scattering of the sonar signal sound energy by the sea floor and sea surface, which can cause *false alarms*. If reverberation levels are higher than ambient noise levels, we speak of a *reverberation limited environment*.

Figure 1 shows a bi-static scenario. As explained, the source and receiver are spatially separated. The receiver can also be a static hydrophone, or hydrophone array, but in this scenario an AUV towing a hydrophone *line array* is shown. When the AUV receives the echo from the target, it can calculate at what *bearing* (angle between towed array heading and target), and at what *range* it thinks the target is, given that it knows where the source was at the ping time, thus creating a bearing-range *contact*. Contacts can be fed into a tracker, for example based on a Kalman filter [4], that combines (spatially) related contacts over time, producing *tracks*. These tracks give a better estimate of the true object’s position

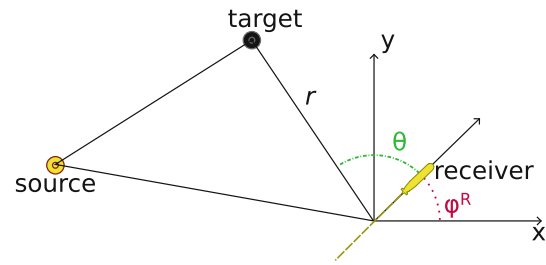


Fig. 1 A bi-static source–target–receiver example, where x and y are the coordinate system, r is the range between target and receiver, and θ is the bearing between the array heading ϕ^R (as measured counter-clockwise from the x axis) and the target

and/or movement, and the uncertainties related to the measurements.

Hydrophone line arrays are not capable of *port–starboard discrimination*. Each sonar signal that is received can be processed to determine its bearing and range, but it is not possible, without further actions, to determine at what side of the array it was received. Therefore, every received contact is interpreted as two contacts: one on each side of the array, referred to as *true* and *ambiguous* contacts. By maneuvering the array, for example by turning a certain amount to port or starboard, the ambiguous contact’s geolocation is seen to move significantly, whereas the true contact’s geolocation remains the same. If the contacts are fed to a tracker, this discontinuity of the geolocation of the ambiguous contact may be exploited to attempt to break a track made on the ambiguous contact.

The term *broadside* refers to the target bearing relative to the hydrophone array. In the case of a vehicle towing an array straight behind it, broadside is 90° relative to the heading of the vehicle. When a target is at broadside to the array, the full aperture of the array is applied to resolve the bearing, which gives the highest bearing resolution. Conversely, a target at or near *endfire*, i.e. directly behind (bearing 180°) or in front of (bearing 0°) the array, will have a poorly resolved bearing due to the poor bearing resolution [22, 37]. For that reason, it can be concluded that an optimal action for an AUV towing a hydrophone line array would be to move so as to get a detected target broadside to its array. When a target is static, one would thus expect a moving receiver to circle the target. When a target is moving, results will depend upon the relative speed differences between target and receiver. But even when an AUV can close in on a target, it will not be expected to do so in a straight line towards it, because that would get the target at endfire. These static and moving target scenarios are explored in this research.

There are both opposing and supporting arguments for the use of underwater vehicles for undersea surveillance, compared to traditional methods. Advantages have been mentioned at the beginning of this section. The challenges or

limitations of AUVs at the moment are their limited endurance, the severely limited underwater acoustic communications, and the limited on-board processing power. The lack of on-board processing power makes it challenging to perform processing at the same level of capability and sophistication as is carried out on currently used platforms. Yet it needs almost the same level of capability to be able to measure its environment through its sensors in order to adapt on the acquired information while performing its mission. The limited bandwidth and limited range of underwater acoustic communications put severe constraints on communication capabilities, whether implicit or explicit. This limits external control, data sharing between vehicles and data sharing with the command and control centre, as well as collaboration approaches. All these limitations need to be overcome to be able to reliably use AUVs in operational scenarios.

1.2 Related work

Mine countermeasures and port protection are other forms of littoral (undersea) surveillance. Eickstedt and Schmidt [16] describe the use of AUVs and low-frequency active sonar for mine countermeasures. Initial results are given for a single vehicle scenario, where on-board processing takes place using mono-static sonar. Potential other applications for AUVs in marine robotics include oceanographic measurements, pipeline inspection, and sea-floor mapping. Research into all these areas is also growing and includes subjects such as path planning [27,34,39], cooperative localization [2,18,41,42], and simultaneous localization and mapping (SLAM) [5,17,25,33,40].

There have not been many publications regarding applications of AUVs for ASW, especially concerning the use of active sonar. Early work at the Naval Postgraduate School (NPS) describes the use of AUVs for target (torpedo) interception and docking [23]. However, the work described seems to be simulation-based only. Target and AUV speeds of 50 knots are reported, which are unlikely given the currently available AUVs [1,24].

Our collaborators at the Massachusetts Institute of Technology (MIT) have published about autonomous vehicles using passive sonar for ASW, for example on improving target tracking through bearing stabilization [36], and demonstrating a concept for multi-vehicle passive target tracking and classification using autonomous surface vehicles [14,15].

Another example of utilizing AUVs for target localization is the work done at Virginia Tech [20,31]. Again, this seems to involve only passive processing, as the vehicles operate on an acoustic source [source level (SL) not mentioned] and have bearing-only sensors. Active processing would imply having range measurements as well. Results are reported of one field trial with two vehicles. The vehicles share informa-

tion when possible, and keep an estimate of the other vehicle's location, sensor output and target estimate, called the "local observer". This allows them to optimize the combined target localization.

Previous research in AUVs for ASW thus seems to mainly address the use of passive processing. However, as outlined in Sect. 1.1, passive sonar may not be sufficient for finding current and future types of submarines in littoral waters. To the best of the authors' knowledge, our 2009 sea trial demonstrated for the first time at sea the use of active sonar signal processing on board an AUV for ASW. Furthermore, the acquired contacts were used by a simple heuristic behavior [21]. Results showed similar observable behavior as the aforementioned experiments by Virginia Tech.

This paper discusses the developments for and experiments performed at the 2010 sea trial, GLINT10 (where GLINT is an acronym for Generic Littoral Interoperable Network Technology.). The on-board signal processing suite has been extended and behavior complexity increased. For the 2010 sea trial, the goal was to demonstrate that AUVs are not only capable of extensive real-time on-board signal processing up to a track level, but also of doing complex calculations on the acquired information in order to change its movements. This would further increase the AUV's situational awareness and adaptivity, taking the first steps to making them available for high complexity missions in high complexity environments that require fully autonomous agents.

The next section, Sect. 2 will describe the equipment used. Section 3 describes the internal workings of our AUV and its autonomy middleware. Section 4 describes the on-board signal processing capabilities and Sect. 5 the adaptive behavior that were developed. Section 6 describes the scenarios that were tested, and the simulation environment. The last two Sects. 7 and 8 provide sea trial results per scenario, and a discussion of these results as well as research aims for the future.

2 Equipment

Two Ocean Explorer (OEX) AUVs were used, shown in Fig. 2. These vehicles are approximately 4.3 m long and 0.53 m wide (21"), currently with a maximum endurance of 7 h at a speed of 1.2 m/s (2.3 kts). Their maximum operating depth is 300 m. Their navigation suite uses a fusion of inertial navigation and a velocity estimate provided by an acoustic Doppler velocity log (DVL). The DVL requires the AUV to operate within a maximum distance of 200 m above the bottom in order to maintain bottom lock. For this reason operations in areas with a water depth of around 100–150 m are currently preferred. Whenever the AUVs are underwater, communications to the command and control centre can only take place through underwater acoustic communica-

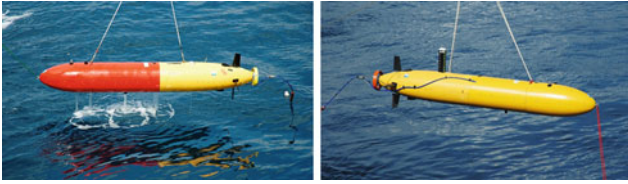


Fig. 2 The two OEX AUVs during deployment and recovery

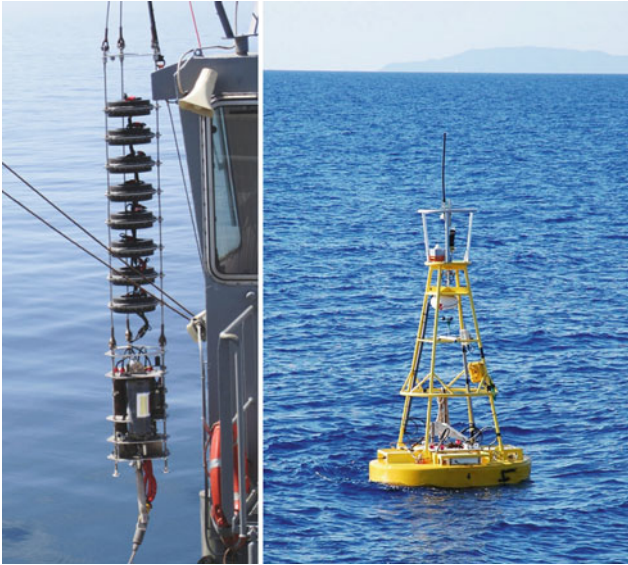


Fig. 3 *Left* the DEMUS source during deployment; the eight free-flooded ring transducers are clearly visible. Underneath the rings are the electronics. *Right* the DEMUS radio buoy

tions. Therefore, each vehicle contains two acoustic modems; an EdgeTech modem in the legacy navigation pressure vessel, and a Woods Hole Oceanographic Institution (WHOI) μ Modem [19].

The OEX AUVs were both deployed with the BENS slim towed array (SLITA) [32]. The arrays are deployed approximately 3.5 m behind the vehicle. The BENS arrays have three nested sets of 32 hydrophones each. The hydrophone set used during the described experiments was optimized for frequencies up to 3.47 kHz (21 cm spacing). One of the towed arrays has four triplet sensors, which allow for port-starboard discrimination, but these sensors were not used at this time. Therefore neither vehicle had the ability to discriminate the starboard from port side measurements. To aid in the geolocation of the array behind the AUV, array navigation data, also referred to as *non-acoustic data* (NAD), from compasses, pitch sensors, and depth sensors was collected on each array.

For the active sonar experiments, the Deployable Experimental Multi-static Undersea Surveillance System (DEMUS) source, shown in Fig. 3, was used. This source is bottom-tethered and was not moved during the experiment. The source transmitted a 2.6–3.0 kHz hyperbolic frequency modulated



Fig. 4 Our echo repeater, used to simulate an underwater target

(HFM) sweep, with a duration of 1 s, a 210 dB SL, and a 12 s ping repetition rate. The DEMUS source was equipped with a WHOI μ Modem to enable remote actuation via underwater acoustic communications, and a radio buoy to allow wireless actuation and monitoring of the source, as well as GPS synchronization for timing and accurate positional estimates.

All assets were deployed from the NATO Research Vessel (NRV) Alliance and the Coastal Research Vessel (CRV) Leonardo. The NRV Alliance served as the command and control centre during the experiments, while the CRV Leonardo deployed an *echo repeater* for simulating a target (Fig. 4). Before algorithms are tested with real targets, it is good practice to try the missions with a simulated target first, as further discussed in Sect. 8. The echo repeater recorded the waveforms received following the DEMUS transmissions, for re-transmission with a user-specified *amplitude gain* after a user-specified delay. During the GLINT10 sea trial experiments described in this document, the echo repeater re-broadcasts the incoming sonar signal with a 20 dB (high) gain over the received level, for the first two experiments. A gain of 15 dB (medium high) was used for the latter two experiments. These amplification levels served as a substitute for the target's sonar *cross-section* or reflectivity. The echo repeater's delay was 2 s, and its deployment depth was 50 m.

3 Vehicle control

The OEX vehicles are controlled via a frontseat–backseat paradigm, as shown in Fig. 5. There are two computers on each vehicle: the *frontseat* computer supplied by the manufacturer, and the *backseat* computer, also known as the *payload* computer, that contains the on-board signal processing, other related processes, and the autonomy middleware. The backseat provides the frontseat with desired speed, heading and depth commands. The frontseat attempts to execute the navigation commands desired by the backseat and also passes back the current navigation estimates.

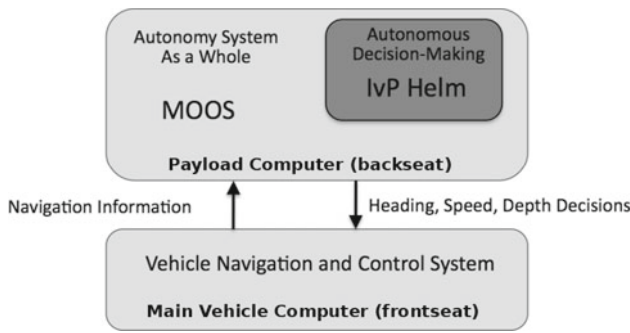


Fig. 5 The frontseat–backseat paradigm as used in MOOS-IvP. The key idea is the separation of vehicle autonomy from vehicle control [8]

The MOOS-IvP middleware developed at the MIT, the University of Oxford, and the Naval Undersea Warfare Center (NUWC) [8], was used as the autonomy middleware and as a framework for inter-process communications. The MOOS or Mission Oriented Operating Suite is open-source middleware that is based on a publish-subscribe architecture [8]. The central ‘server’ application is called the MOOSDB. Although not an actual database, it can be seen as an information buffer that holds the current state of variables provided by or required by all the on-board signal processing, communication, navigation, and autonomy processes. Processes can subscribe to and/or publish variables to the MOOSDB in order to exchange information. This approach is attractive, because it is not necessary to write custom communication interfaces between the processes. It is also useful because the contents of the MOOSDB at any time can be logged. These logs can be examined forensically for debugging and mission analysis.

The IvP helm is a MOOS application that enables behavior-based autonomy. Behaviors can run simultaneously and can be grouped into behavior sets, which are active based on certain conditions. Each behavior is given a weight which is defined at mission start but may also be adjusted dynamically during the mission by on-board processes. IvP, a mathematical interval programming technique, combines the objective functions produced by active behaviors to determine a globally optimal solution for each domain [7,8]. Objective functions can be implemented over any of (in our case) three domains: speed, heading and depth. Because the IvP search is not only optimal but also fast, it is suitable for in-the-loop control, at typically four iterations per second, to determine the desired navigation commands.

4 On-board processing

Given that the AUVs must be able to react to a developed understanding of the underwater scene, they need to be capable of on-board processing and interpretation of the output of their sensors, principally their towed array. This on-board

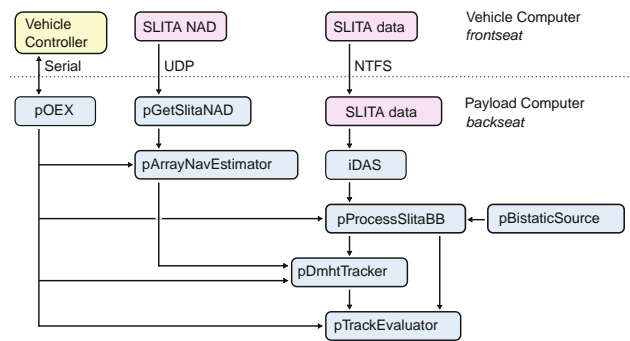


Fig. 6 The OEX’s active sonar on-board processing chain

processing takes place on the payload (backseat) computer. The MOOS processes that make up the active sonar signal processing suite are linked together as shown in Fig. 6. There are three main streams of data flow:

- pOEX is the process that receives vehicle navigation as well as conductivity, temperature and depth (CTD) information from the front-seat computer, via a serial line. This is parsed and published to the MOOSDB.
- pGetSlitaNAD and pArrayNavEstimator, respectively, acquire and process the towed array’s NAD, the data from the navigation sensors in the array. These include heading, depth and pitch information (see Sect. 2). pGetSlitaNAD acquires the raw NAD via UDP and parses it. pArrayNavEstimator uses the parsed NAD together with the vehicle’s navigation information, to estimate the shape, location and heading of the array at the time of a measurement. This is needed by the tracker to geolocate the processed contacts.
- iDAS, the digital acquisition system interface, monitors whether a new data file with the towed array’s acoustic data has been written. If so, pProcessSlitaBB processes this data up to contact level. The contacts produced by pProcessSlitaBB are input to pDmhtTracker which publishes tracks. Tracks are subscribed to by pTrackEvaluator that ranks them according to the scheme described below.

pProcessSlitaBB pProcessSlitaBB is a MOOS front-end to the active sonar signal processing algorithms libraries. It includes standard active sonar processing elements [26];

- beamforming: the time series on each of the towed array’s hydrophones is mathematically transformed in such a way as to produce a time series per look direction (*beam*),
- matched filtering: for each beam, the time series is filtered using a replica of the source’s outgoing pulse, resulting in a pulse-compressed time series,

- contact formation: down each beam the matched filter output is normalized to be able to calculate the SNR per point, then a SNR threshold is applied to the normalized data to form detections.

The libraries used are computationally optimized versions of algorithms previously developed at our institution [3,21,28] and by collaborators at the MIT [30]. The resulting contacts are published to the MOOSDB in XML format, to which `pDmhtTracker` subscribes.

pDmhtTracker Our distributed multi-hypothesis tracker (DMHT) processes the contacts and generates tracks [11,12], as introduced in Sect. 1.1. In our real-time usage of the DMHT, the multi-hypothesis and distributed facilities are currently not utilized. This essentially reduces the tracker to an extended Kalman filter [4], with facilities for controlling track birth/death and contact/track association [11]. The tracker also internally computes the geolocation using the contact’s range and bearing, source location, array location and array heading. Information on all tracks are published as a track report to the MOOSDB in XML format.

pTrackEvaluator The track report, containing all active tracks per ping, is subscribed to by `pTrackEvaluator`. The track evaluator counts the amount of tracker report updates (`cntUpdates`), and waits until it reaches the pre-set `numTracksUpdates`¹ number of track updates before taking action.

As has been explained in Sect. 1 the towed arrays cannot discriminate whether a contact is detected on the port or starboard side of the AUV. Both true and ambiguous contacts are passed into the tracker. Therefore, it is not desirable to act on the first track formed by the tracker, which with a 50% probability may be tracking the ambiguous contact. Instead it is advisable to try to break the track associated with the ambiguous contact. To this purpose, `pTrackEvaluator` switches the mode (as further explained in Sect. 5) to `DISAMBIGUATE` and waits again for `numTracksUpdates` updates. It then assumes that tracks associated with the ambiguous contacts have been broken, and switches the mode to `OPTIMIZE`. The optimization behavior then becomes active. Algorithm 1 shows the algorithm in `pTrackEvaluator` in pseudocode.

An empirical approach is taken to track ranking, no target model is used yet for classification. Instead, track ranking takes place under the assumption that the associated contact is expected to have a high SNR, which was the case for all experiments during GLINT10. Furthermore, because it is

¹ The `numTracksUpdates` parameter can be set to any integer value the operator might find desirable, the default is 15.

Algorithm 1 `pTrackEvaluator`

```

getAllTracks();
rankAllTracks();
if cntUpdates ≤ numTracksUpdates then
    TRACKS = false // wait
else if cntUpdates ≤ numTracksUpdates * 2 then
    TRACKS = true
    MIRROR_TRACKS = true // start disambiguating
else
    TRACKS = true
    MIRROR_TRACKS = false // start optimizing
end if

```

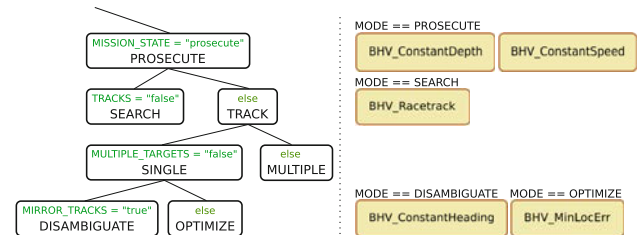


Fig. 7 Behavior modes and active behaviors

assumed that the ambiguous tracks are broken by the disambiguation maneuver, track length can also be used as a cue to determine whether a track is of interest. The track ranker, (`rankAllTracks()`), combines the SNR of the last associated contact and the length of the track. A moving average of the SNR data is kept for every track, using an exponentially fading filter with a *half-life time* of 60 s, which is augmented at every tracker update. The averaged SNR is added with unit weight to the length of the track, to create a composite track score. A list of track identification numbers and their scores is published to the MOOSDB, where it can be subscribed to by downstream processes and behaviors.

5 Behaviors

Figure 7 shows the behavior modes and the behaviors acting on those modes, as set up for GLINT10. At each iteration of the IvP helm, variables in the MOOSDB are evaluated to determine the current mode. The modes can be seen as the state spaces defining what behaviors will be active on the vehicle [8], and thus generally are the action-selection mechanism, describing the scenario and mission for the AUV. In the current set-up, the mode changes within the prosecute state are controlled by `pTrackEvaluator`, which changes the variables that are monitored to determine the mode. Additionally, a mode change can also be brought about by endflags of certain behaviors, other processes, or forced if an operator sends an acoustic message to the vehicle setting certain variables.

Modes can be set up in a hierarchical fashion to allow more general behaviors to be running irrespective of certain specific behaviors. As Fig. 7 shows, this hierarchy is used to run

a constant speed and constant depth behavior whenever the AUV is prosecuting (MODE == PROSECUTE), e.g. acquiring and processing the active sonar data. However, depending on what it has been processed so far, different heading behaviors are active at different times.

At the beginning of a mission, when the AUV starts processing, but has not yet made any tracks, or at any other time when the AUV has lost all tracks, the AUV is in a search mode (MODE == SEARCH). After forming tracks, the AUV switches to disambiguation mode (MODE == DISAMBIGUATE), as explained in Sects. 2 and 4. After disambiguation, the AUV assumes it can now optimize for a single true track, i.e. it assumes that the ambiguous contact's track has been broken. At this point it runs the behaviors that activate on the optimization mode: BHV_MinLocErr.

Because all aforementioned modes (search, disambiguate and optimize) are submodes of the prosecute mode, all behaviors whose activation conditions fire on the prosecute mode (BHV_ConstantSpeed and BHV_ConstantDepth) are still active, as well as possible behaviors operating on even higher level modes [8]. BHV_MinLocErr will be described in detail in the next section, the other behaviors listed in Fig. 7 are, in short:

- BHV_ConstantDepth: drive the vehicle at a specified depth [8].
- BHV_ConstantSpeed: drive the vehicle at a specified speed [8].
- BHV_ConstantHeading: drive the vehicle at a specified heading [8].
- BHV_Racetrack: drive the vehicle along a (rectangular) racetrack. The user can specify track location, orientation, length, width, the distance-to-track-line tolerance, the angle at which to approach the racetrack, speed, and whether or not it should be traversed clockwise.

During the described missions, at any given time, a couple of additional behaviors were active for vehicle safety. These (standard IvP) behaviors are [8]:

- BHV_OpRegion: a user-defined 2-D boundary box given by a convex polygon, overall timeout, maximum depth, and minimum altitude. If any of these are violated, all speed, depth and heading commands are set to zero.
- BHV_MemoryTurnLimit: limit the amount of turn possible per iteration, to avoid vehicle turns that may cross its own path (n.b. useful for towed array safety).
- BHV_AvoidObstacles: 2-D obstacle avoidance for (usually pre-defined and sta-

tic) obstacles. Obstacle avoidance distances are user-defined parameters.

- BHV_AvoidCollision: 3-D collision avoidance for (user-defined or acoustically received) contacts. Collision avoidance distances are user-defined parameters.
- bhv_abort: a combination of a waypoint and constant depth behavior for safe abort to a user-defined waypoint, followed by a combination of a go-to-depth and constant speed behavior for surfacing.

5.1 BHV_MinLocErr

BHV_MinLocErr aims to minimize the error in localization of a track, thus optimizing the AUV's position for optimal target localization. A localization error covariance matrix is constructed from the estimated target position variances, and the x and y target estimate covariance, as derived in [10]. The optimization measure, which needs to be a maximization function, is the inverse of the trace of the localization error matrix:

$$\left(\text{tr} \left(\begin{bmatrix} \sigma_{xT}^2 & \sigma_{xTyT} \\ \sigma_{xTyT} & \sigma_{yT}^2 \end{bmatrix} \right) \right)^{-1} = \frac{1}{\sigma_{xT}^2 + \sigma_{yT}^2} \quad (1)$$

The necessary variances over x and y for a given track can be calculated, as [10]:

$$\begin{aligned} \sigma_{xT}^2 &= \sigma_{xR}^2 + \cos^2(\theta + \phi^R) \sigma_r^2 \\ &\quad + r^2 \sin^2(\theta + \phi^R) (\sigma_\theta^2 + \sigma_{\phi R}^2) + 2 \cos(\theta + \phi^R) \sigma_{xRr} \\ &\quad - 2r \cos(\theta + \phi^R) \sin(\theta + \phi^R) (\sigma_{\theta r} + \sigma_{\phi Rr}) \end{aligned} \quad (2)$$

$$\begin{aligned} \sigma_{yT}^2 &= \sigma_{yR}^2 + \sin^2(\theta + \phi^R) \sigma_r^2 \\ &\quad + r^2 \cos^2(\theta + \phi^R) (\sigma_\theta^2 + \sigma_{\phi R}^2) + 2 \sin(\theta + \phi^R) \sigma_{yRr} \\ &\quad + 2r \sin(\theta + \phi^R) \cos(\theta + \phi^R) (\sigma_{\theta r} + \sigma_{\phi Rr}) \end{aligned} \quad (3)$$

where (see Fig. 1)

- θ is the measured bearing,
- ϕ^R is the array heading,
- r is the range between target and receiver,

and

- σ_{xR}^2 and σ_{yR}^2 are the variances in measured receiver x and y positions,
- σ_r^2 is the variance in range between target and receiver,
- σ_θ^2 is the variance in measured bearing,
- $\sigma_{\phi R}^2$ is the variance in measured array heading,
- σ_{xRr} and σ_{yRr} are the covariances between, respectively, receiver x or receiver y position error and the target-receiver range error,

Table 1 BHV_MinLocErr parameters: measurement uncertainties

Parameter	Default input value
σ_{source}	15,15,0 (m)
σ_{receiver}	15,15,0 (m)
$\sigma_{\text{endfire_width}}$	18.2 ($^{\circ}$)
$\sigma_{\text{arrayheading}}$	1.0 ($^{\circ}$)
$\sigma_{\text{propagationtime}}$	0.1 (s)
$\sigma_{\text{soundspeed}}$	7.5 (m/s)

Standard deviations are related to the towed array's characteristics, except for the standard deviation on sound speed

- $\sigma_{\theta r}$ is the covariance between bearing error and target–receiver range error,
- $\sigma_{\phi R r}$ is the covariance between array heading error and target–receiver range error.

To calculate these variances, not only are the receiver position, source position, and estimated target position necessary, but also the variances in all of these, as well as variances in sound speed, and propagation time [10]. Table 1 shows the behavioral parameters, used during GLINT10. These are guided either by the characteristics of the towed array or the source waveform, see Sect. 2. Part of these parameters, such as the variance in target–receiver range and the variance in the bearing, need to be dependent on the SNR at the target range and azimuth. The SNR, for adapting these parameters for future predictions, is calculated using a simple equation that combines SL, target strength and the relative geometries of the source, target and receiver [9, 38]. Parameters not listed in Table 1 are either calculated or retrieved from the MOOS-DB, published there by on-board processes such as pOEX.

The behavior parameters can influence the size of the localization error, because they determine the size of the errors in the measurements. However, changing the parameters would not change the general shape of the function, nor where its maxima lie. Changing $\sigma_{\text{endfire_width}}$ can change the smoothness of the error localization function, but again, maxima will remain in the same location. The most dominant terms that determine the localization error function are the directivity of the towed array (broadside is best, endfire worst, see Sect. 1.1), and the *blanking region*, i.e. the area where the target is between source and receiver and thus cannot be detected. Range, and as a consequence the strength of the target response, is of much less significance to the localization error than the array directivity. Therefore it can be expected that the vehicle will mostly try to keep any target at broadside to its array, to get the most accurate localization.

At each iteration of the IvP solver, which as a default is four times per second, Eq. 1 is calculated for the lay-outs that could be expected at the next ping time, for all possible headings that the AUV can take at the current time. Heading

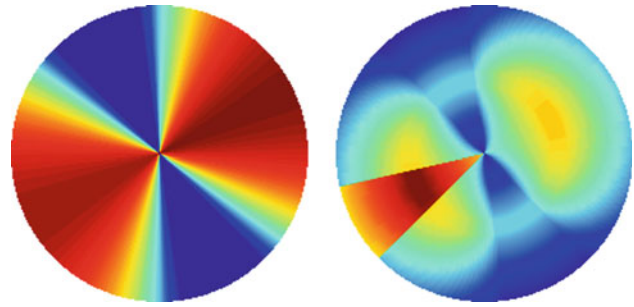


Fig. 8 Individual BHV_MinLocErr (left) and collective (right) objective functions plots from IvP, taken while the AUV is optimizing. Red (around 65 and 235 degrees in the individual plot, and the slice around 240 degrees in the collective plot) equals high preference and blue (around 155 and 335 degrees in individual and outer boundaries of collective plot) equals low preference. Speed is displayed along the radius, heading in 360° , depth is not shown

values are varied between 0° and 360° , using 0.5° increments. It is assumed that the AUV can change to these headings at the current time, and then follow a straight movement at the current velocity to the next ping position. The resulting objective function only affects the AUV's heading, and is therefore used in combination with constant speed and constant depth behaviors, as explained at the beginning of this section. Note that even though the AUV's speed could potentially be varied, given the 1.2 m/s maximum speed of the vehicle and the fact that the AUV needs to operate at least at 0.7 m/s to properly tow the array, the potential benefits of a speed behavior at this time are believed to be minimal.

Figure 8 shows the objective functions used by IvP to determine the desired speed (along the radius) and heading (angle). The left figure shows the objective function created by BHV_MinLocErr, which as mentioned above has no speed sensitivity. The fundamental ambiguity due to the equal localization error when holding the target on broadside, either to the port or starboard side, to its towed array, is clearly visible. The right figure shows the collective objective function that is created by IvP. For this example, the collective function consisted of the BHV_MinLocErr, a constant speed behavior, constant depth behavior, and a turn limit behavior. The turn limit behavior [8] limited the desired heading change to plus or minus 15° of the current heading. For the experiments described in this paper, this behavior has a weight of 200 versus a weight of 100 for the other active behaviors, and thus has a profound effect, as can be seen by the raised slice in the collective objective function plot.

6 Scenarios

In June/July 2009 and July/August 2010, the GLINT09 and GLINT10 sea trials were held. Both trials were held in the Tyrrhenian Sea, south of the island of Elba and north of Porto Santo Stefano. This area is suitable for our AUV operations

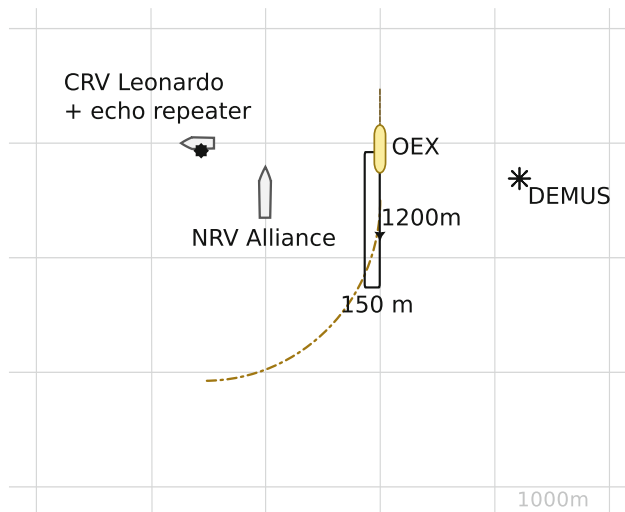


Fig. 9 Static target scenario with anticipated AUV movement. The OEX starts in a southbound racetrack, the ‘target’ (CRV Leonardo + echo repeater) is static, as are the NRV Alliance and the DEMUS source. Grid size 1,000m

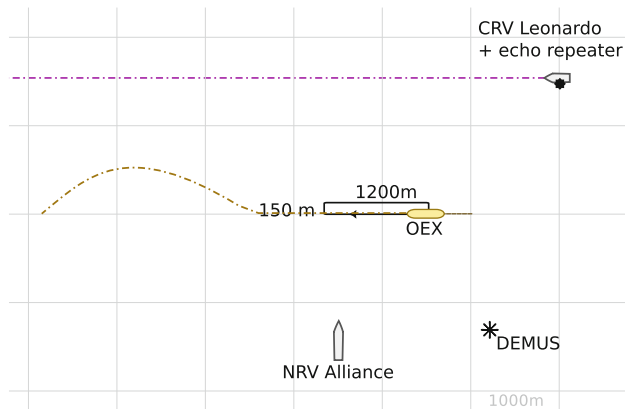


Fig. 10 Dynamic target scenario with anticipated AUV and ‘target’ movement. The OEX starts in a westbound racetrack, the ‘target’ (CRV Leonardo + echo repeater) starts to the northeast in a westbound movement. The NRV Alliance and DEMUS source are static. Grid size 1,000m

because of its relatively flat bathymetry and its shallow water depth of approximately 110 m. As the experiments performed during GLINT09 have been described in [21], we focus here on technologies and approaches developed within the past year, as well as the results obtained during the GLINT10 experiment.

The goal during the GLINT10 sea trial was to demonstrate the minimize localization error behavior at sea for two scenarios, preceded by consistent demonstrations in simulation. The scenarios were: (1) optimizing for a static target, and (2) optimizing for a moving target. Figure 9 shows the setup for the static target scenario, and Fig. 10 for the moving target scenario. In all cases the DEMUS source was static (bottom-mounted), as was the NRV Alliance, which had the command and control centre on board.

The general content of each experiment was as follows: the AUV (either one of our two OEXs) would start the experiment driving in a racetrack pattern. This is a rectangular run with, for example, a length of 1,200m and a width of 150m. Then the source would be turned on and in the case of the moving target scenario, the target (CRV Leonardo + echo repeater) would start to move on a straight line course. The AUV would then process the active sonar data, and after the predefined number of updates, make the disambiguation movement. The disambiguation behavior was a simple constant heading behavior that changed the heading to the current heading plus or minus a present angle (default 30°). After following the disambiguation heading for the same number of track updates, it would start optimizing for the highest scored track for 30 min, before returning to its start position. The mode changes were initiated by pTrackEvaluator, as explained in Sects. 4 and 5.

6.1 Simulation environment

The simulation environment consists of:

- all processes that run at a field trial, i.e. the on-board processing suite, and all behaviors that will be used,
- MOOS-IvP processes for viewing the simulation,
- MOOS-IvP processes for simulation of hardware not present, for example a vehicle simulator, an acoustic modem simulator, a target simulator, etc.,
- an acoustic data stimulator.

The acoustic data stimulator generates time series level acoustic data files, as a substitute for the real acoustic data normally received on the towed array. A simple data stimulator was used that simulates direct blast and target returns (including direction of arrival on the array and transmission loss based on a simple spreading model), white Gaussian background noise, and additional bandlimited, exponentially decaying white Gaussian noise for reverberation.

7 Results

Results were obtained for both the static and moving target scenarios. Sections 7.1 and 7.2 describe the results obtained from the sea trial, and provide comparisons with simulation results per scenario. Behavior performance as well as tracker performance is discussed.

7.1 Optimizing for a static target

During GLINT10, optimization for the static target was demonstrated at sea three times. Figure 11 shows a screenshot

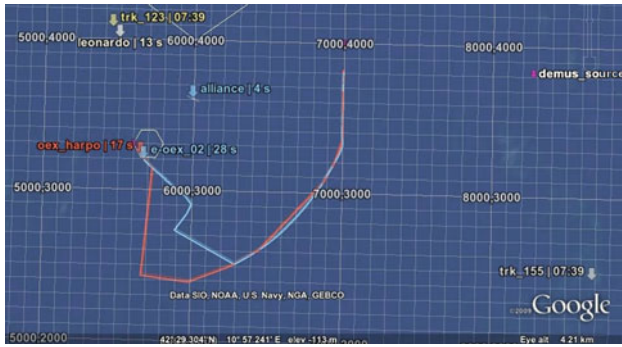


Fig. 11 Command and control centre (alliance) display, third demonstration static target; the AUV (oex_harpo/e-oex_2) is optimizing for a static target (leonardo), using on-board active sonar processing (source: demus_source). The AUV’s position updates are received via two acoustic modems, indicated by e-oex_2 (light blue) and oex_harpo (red). trk_*’s are tracks sent from the AUV via acoustic communications to the command and control centre display. Grid size 100 m

from the command and control centre for the third demonstration of the OEX optimizing on the static target. The OEX started in a north to south racetrack from approximately [7000, 4000], going 1.0 m/s. After approximately 10 min, the DEMUS source was turned on, and the OEX started active sonar processing. After 15 updates from the tracker, the OEX added 30° to its current heading for disambiguation. After following the ‘disambiguate’ heading for another 15 track updates it started optimizing. All the while, the CRV Leonardo was simulating a static target at [5500, 4000] using the echo repeater. Figure 11 shows that the OEX made a circular movement around the CRV Leonardo.

Discrepancies between the red and blue AUV paths displayed are due to lags in the status updates received through the acoustic communications from the two separate acoustic modems. The OEX actually went to a point a little south of the most south-west point on the red path, then started returning to the start position, receiving an update on the blue path, but was then sent to a loiter. At the loiter location updates were received again from both modems.

Table 2 shows the tracker performance for the three experiments. Performance during the first two experiments was not as good as for the third experiment. For the first demonstration, the payload computer was not receiving the towed array’s navigation data from the vehicle computer, because of a configuration error on the front-seat computer. In such a scenario, as a fall-back, the array heading is estimated using a time-delayed version of the vehicle heading (‘worm-in-a-hole motion assumption’). Thus, errors in array heading estimation are likely to have decreased tracker performance. Overall, the tracker still got the right track 96.64% of the time the AUV was optimizing. Configuration was double-checked for future experiments to prevent the same error from happening again.

Table 2 Tracker performance at sea for the static target scenario

	Amount	Percentage
Experiment 1		
Unique tracks formed	37	
Tracks followed	7	
Track followed on target (updates)	144/149	96.64
Track followed off target (updates)	5/149	3.36
Experiment 2		
Unique tracks formed	40	
Tracks followed	10	
Track followed on target (updates)	133/149	89.26
Track followed off target (updates)	16/149	10.74
Experiment 3		
Unique tracks formed	36	
Tracks followed	1	
Track followed on target (updates)	149/149	100
Track followed off target (updates)	0/149	0

A track is ‘on target’ when it was (mostly) within 500 m of the target’s position

For the second demonstration, more ‘wrong’ tracks were followed than in the previous demonstration. Although still approximately 89% of the followed tracks were on the target, performance severely degraded in comparison to the other two at-sea demonstrations. Post-mission analysis showed that this degraded performance was due to a problem with noise level estimates in the signal processor’s detector. High range sidelobes of the loud target signal contaminated and increased the background noise estimate near the direction of arrival. These range sidelobes were not present, or below reverberation levels, for directions away from the direction of arrival. When the data was normalized with these noise estimates, the data near the direction of arrival was suppressed by the over-estimated noise, but data off the direction of arrival was not. The result was a flattening of the main lobe on the direction of arrival leading to a poor bearing estimate. We mitigated this effect during the sea trial by decreasing the echo repeater’s amplitude gain from 20 to 15 dB. Detectors are an active area of research, and this continues to be explored in our research as well as different methods of normalization, see Sect. 8.1, to prevent such errors for future experiments.

Once the echo repeater’s amplitude gain was decreased, tracker performance for the third demonstration was, from a behavioral perspective, optimal. 100% of the time that the AUV was optimizing, it followed the same track, which was near the target.

Sea trial versus simulation results for a static target The performance of the behavior was tested many times in simulation, to demonstrate robustness and consistent performance, before it was tested at sea. The experiments at sea were done

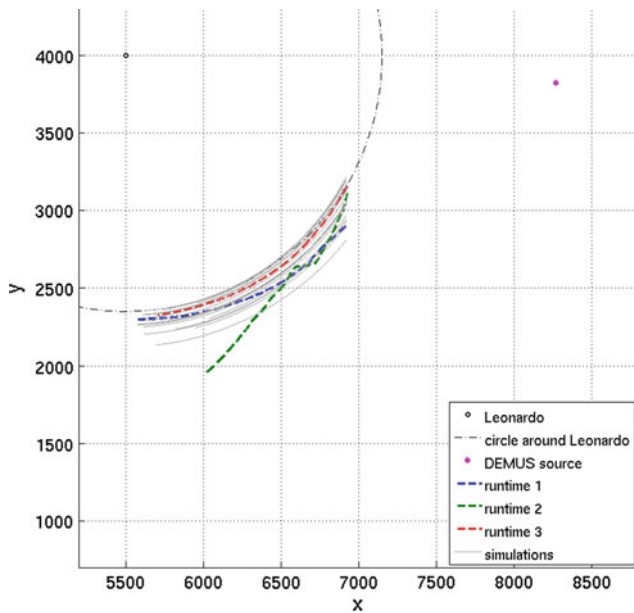


Fig. 12 Overlay of field demonstrations on simulation results for the static target scenario. Inter-simulation differences are due to differences in start time of the data stimulator

to demonstrate performance under real conditions. Twenty simulations were done for each scenario. For all static target simulations the same set-up and settings were used, but the starting time of data stimulation (and thus data acquisition) was varied, because this was a factor most likely to be different during the field trial. Different start times lead to different layouts of all assets at the time the AUV starts acquiring, tracking and optimizing, therefore this was varied for robustness testing. Over the 20 simulations, the mean start time was 590 s, with a standard deviation of 114 s. Given that the AUV was going 1.0 m/s, the standard deviation for the AUV’s position was 114 m.

Figure 12 shows the sea trial performance and simulation results for a static target in one plot. The 20 simulation results are shown in dotted light gray, versus dashed colored paths for the at-sea experiments. For the 20 simulations the amount of unique tracks formed had a mean of 4.05 with a standard deviation of 1.47. The amount of tracks followed had a mean of 1.05 with a standard deviation of 0.22.

Figure 12 shows that in simulation the AUV basically makes a perfect circle around the static target. For illustration purposes, a semi-dashed black circle has been drawn around the target position (at a radius of approximately 1650 m). In the first two demonstrations, tracks broke and new tracks formed at different locations, in the case of the second experiment even at the ambiguous track’s location. In those cases the performance was not as good as for the third demonstration where there were no problems with tracker performance. In the third demonstration, the AUV followed one track near the actual target position for the whole time it was optimiz-

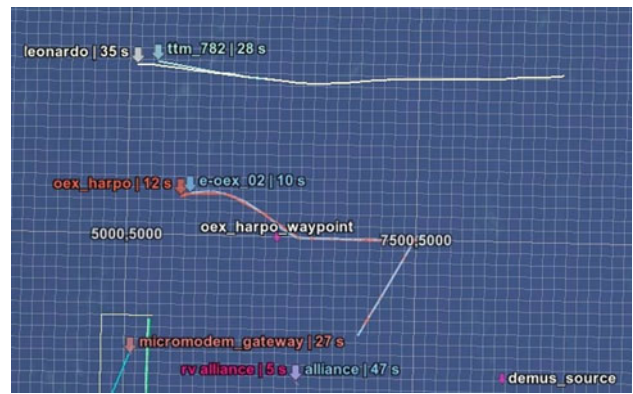


Fig. 13 Command and control centre (alliance) display, first demonstration moving target; the AUV (oex_harpo/e-oex_2) is optimizing for a moving target (Leonardo), using on-board active sonar processing (source: demus_source). The AUV’s position updates are received via two acoustic modems, indicated by e-oex_2 (light blue) and oex_harpo (red). ttm_* indications are radar tracks

ing, and performance compares exceptionally well to what was demonstrated in simulation.

The circular behavior is due to the previously explained (Sects. 1.1 and 5) dominance of the towed array’s directivity. The gain that can be achieved in SNR by moving closer does not weigh up to the gain in localization by keeping the target at broadside. If the aim of the experiment is to get the most accurate localization, then the current behavior would do well. However, if there would be a need for the vehicle to zone in on a target, integration of a more precise calculation of SNR could increase the importance of this term and thus allow for the vehicle to do so, as discussed in Sect. 8.1. In addition, one has to realize that the current behavior only looks one ping interval into the future and therefore may not realize the potential gain that could be achieved further into the future, also discussed in Sect. 8.1.

7.2 Optimizing for a moving target

During GLINT10, one field experiment was performed to demonstrate optimization for a moving target. A screenshot of this successful demonstration is shown in Fig. 13. The OEX started in an east to west racetrack from approximately [7500, 5000], going 1.0 m/s. After approximately 15 min, the DEMUS source was turned on, the OEX started active sonar processing, and the CRV Leonardo started moving west-bound from [9000, 6500] at 2.0 m/s towing the echo repeater. After 15 updates from the tracker, the OEX added 30° to its current heading for disambiguation. After following the ‘disambiguate’ heading for another 15 updates it started optimizing.

When the OEX was optimizing it first moved closer to the Leonardo’s track, because it was still ahead as the Leonardo was further east than the OEX. However, as the Leonardo

Table 3 Tracker performance at sea for the moving target scenario

	Amount	Percentage
Unique tracks formed	14	
Tracks followed	1	
Track followed on target (updates)	149/149	100
Track followed off target (updates)	0/149	0

A track is ‘on target’ when it was (mostly) within 500m of the target’s position

drew to the same longitude as the OEX, the OEX started to move in parallel, and as the Leonardo moved ahead, the OEX moved away in an approximately hyperbolic movement, trying to keep the Leonardo at broadside to its towed array.

Table 3 shows tracker performance during optimization. As for the third demonstration in the static scenario, results were optimal from a behavioral perspective. During the AUV optimization period, the vehicle optimized all the time for a track near the actual target, and the track did not break.

Sea trial versus simulation results for a moving target Figure 14 shows the sea trial performance and simulation results in one plot for our AUV optimizing for a moving target. The moving target scenario was also tested for robustness and consistent performance in simulation. Again, 20 simulations were done, and starting times of data stimulation (and data acquisition) were varied. Over the 20 simulations, the mean start time was 777s with a standard deviation of 129s. This corresponds to a standard deviation of 129m in AUV position, and a standard deviation of 258m in the target position, given that the AUV was moving at 1.0m/s and the target at 2.0m/s. For all 20 simulations the number of unique tracks formed had a mean of 4.55 with a standard deviation of 1.15. The number of tracks followed had a mean of 1.00 with a standard deviation of 0.00.

Figure 14 shows the field performance compared to simulations. For all, the target moved from northeast to northwest, approximately 1,500m North of the AUV. All demonstrations show an approximately hyperbolic movement, caused by the dominance of array directivity (towards minimizing localization) over other factors, combined with the higher target speed as the target came alongside and then drove ahead of the AUV. Given the limited speed of the AUV in respect to the target, this may not be undesirable, because it would not be able to catch up with it, as further discussed in the next section.

8 Conclusion

Autonomous off-board sensor systems are attractive candidates to complement high-value assets in undersea surveil-

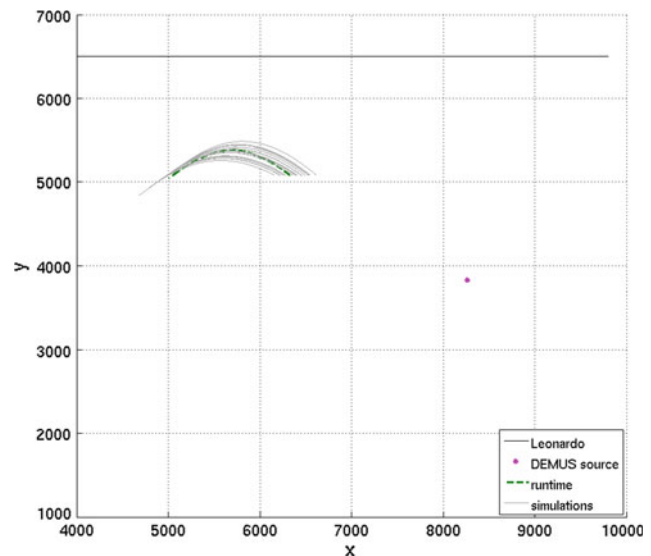


Fig. 14 Overlay of field demonstration on simulation results for the moving target scenario. Inter-simulation differences are due to differences in start time of the data stimulator

lance, among others for the potential to reduce manning, personnel risks, and the ability to integrate them into a scalable, persistent, and cost-effective networked system. AUVs for one, are currently not yet capable of operating autonomously in potentially complex dynamic environments. The limited bandwidth and limited range of underwater acoustic communications put severe constraints on communication capabilities, whether implicit or explicit, increasing the need for high levels of autonomy. To that purpose, their situatedness, adaptivity, and self-sufficiency should be improved. The use of AUVs with on-board passive processing for ASW has previously been addressed, but on-board active sonar signal processing has received little attention.

In 2009, a first demonstration of on-board active sonar signal processing on an AUV for ASW was demonstrated. This encompassed processing up to contact level, and a simple heuristic adaptive behavior. The goals for our 2010 sea trial were threefold:

- to demonstrate the extended on-board signal processing suite,
- to increase behavior complexity, i.e. to be able to do full bi-static calculations on-board the vehicle, at the standard rate of 4 Hz,
- to demonstrate good performance at sea, and compare this to what has been demonstrated in simulations.

These steps would increase the AUV’s situatedness and adaptivity, in order to prepare them for high complexity missions and/or environments.

This paper has described the on-board signal processing including a tracker, and an adaptive behavior, which were

successfully implemented. The resulting system was tested in simulations, showing consistent performance in both a static target and moving target scenario when varying the starting times of data stimulation. Both scenarios were elaborately tested in simulations. Due to both time and cost overhead of sea-going experiments, this is an integral part of our research. Because the data stimulator produced simplified data compared to what could be expected at sea, especially in terms of bottom loss effects and clutter, these results still had to be validated at sea.

During GLINT10 the static target scenario was successfully demonstrated three times, two of them showing potential issues that can be encountered in a real situation. Performance for the third demonstration was comparable to simulation performance. The moving target scenario was only demonstrated once, but was successful, showing good tracker performance and the OEX AUV demonstrating the predicted trajectory.

8.1 Discussion and future work

There were some specific problems that were encountered during the recent at-sea experiments. The first demonstration against the static target suffered from a configuration error. To that purpose, more templates with default values, from which missions files can be generated, will be used. Furthermore, checklists will also be introduced to reduce the likelihood of configuration errors. Following the discussion in Sect. 7.1 regarding the degraded results in the second demonstration, we intend to reduce sidelobe contamination, by experimenting with other noise estimation methods and improving the detector. Another simpler solution to avoid this problem, is to use unnormalized data for estimating the bearing of contacts above a certain level.

Regarding the observable behavior for both the static and moving target, it has yet to be proven whether or not this is the best approach to undersea surveillance. As mentioned in Sects. 7.1 and 7.2, this will depend upon operational goals, as well as upon the capabilities and the amount of assets. Currently, AUVs have limited speed and endurance, which limits their possible usage. The approach was taken to improve target localization, because in the case of a moving target, it was known that there would be little opportunity to actually intercept. The same behavior was for reference tested on a static target first. Why the AUV did not circle inwards to this target is dependent on a couple of factors. For one, as explained, the minimization of the localization was dominated by array directivity and SNR gain had little effect. This could perhaps be made of greater importance by integrating a more comprehensive SNR estimate. Other work has investigated a behavior that has been designed to optimize AUV heading based on maximizing signal excess [29] and plans

are underway to integrate its more comprehensive SNR estimate into `BHV_MinLocErr`.

Secondly, the other issue with the developed behavior, and reactive systems in general, is that the possible gain that can be achieved in the far future, is not considered. The developed behavior only tries to achieve the best possible position and heading it can achieve at the next ping time. However, it may be that it can eventually reach a higher pay-off by going through a locally suboptimal movement. This will also become more apparent when working with multiple vehicles. To that purpose, it may become necessary to introduce more advanced reasoning unto the vehicles, for example to coordinate tasks and allow for a handover. Reasoning may in any case turn out to be necessary to compensate for the lack of knowledge introduced by the limited underwater acoustic communications. Furthermore future research will involve studies on extending behaviors to, or developing them for, the speed and depth domains. Simulation studies should allow for experimenting with potential capabilities of future AUVs, beyond current hardware limits.

Our research has shown that on-board processing can already be performed up to a track level. However, all currently described experiments have been performed on a simulated target with relatively high amplitude gain. The currently used evaluation scheme is empirical, and would most likely not be sufficient against a real target. To acquire more information, the next step in sensor processing will be to include continuous wave (CW) processing. CW processing will lead to Doppler measurements on the contacts, which provide additional clues for classification. Thus we continue our efforts towards developing a heterogeneous sensor network for littoral surveillance.

Acknowledgments This work was funded by our scientific program of work, within the Cooperative ASW project. The authors thank the crew of NRV Alliance and CRV Leonardo for their help in obtaining the at-sea data. Furthermore many thanks go to the great technical assistance and participation during GLINT10 from the staff and students of the Massachusetts Institute of Technology's Laboratory for Autonomous Marine Sensing System (MIT LAMSS), and from the Naval Undersea Warfare Centre (NUWC).

Open Access This article is distributed under the terms of the Creative Commons Attribution Noncommercial License which permits any noncommercial use, distribution, and reproduction in any medium, provided the original author(s) and source are credited.

References

1. Arafat H, Stilwell D, Neu W (2006) Development of a dynamic model of a small high-speed autonomous underwater vehicle. In: Proceedings of the IEEE/MTS Oceans 2006 Conference. IEEE, Boston, MA, USA
2. Bahr A (2009) Cooperative localization for autonomous underwater vehicles. Ph.D. thesis, Massachusetts Institute of Technology and Woods Hole Oceanographic Institution, Cambridge, MA, USA

3. Baldacci A, Haralabus G (2006) Signal processing for an active sonar system suitable for advanced sensor technology applications and environmental adaption schemes. In: EUSIPCO 2006. European signal processing conference, Florence, Italy
4. Bar-Shalom Y, Li X, Kirubarajan T, Wiley J (2001) Estimation with applications to tracking and navigation. Wiley, New York
5. Barkby S, Williams SB, Pizarro O, Jakuba M (2009) An efficient approach to bathymetric SLAM. In: Proceedings of the IEEE/RSJ international conference on intelligent robots and systems (IROS), St. Louis, MO, USA, pp 219–224
6. Benedict JR (2005) The unraveling and revitalization of U.S. Navy antisubmarine warfare. *Nav War Coll Rev Spring* 58(2):93–120
7. Benjamin MR (2004) The interval programming model for multi-objective decision making. Tech. Rep. MIT-CSAIL-TR-2004-058, Massachusetts Institute of Technology, Cambridge, MA, USA
8. Benjamin MR, Newman P, Schmidt H, Leonard JJ (2010) An overview of MOOS-IvP and a users guide to the IvP helm autonomy software. Tech. Rep. MIT-CSAIL-TR-2010-041, Massachusetts Institute of Technology, Cambridge, MA, USA
9. Burdic WS (1991) Underwater acoustic system analysis, 2nd edn. Prentice-Hall, Englewood Cliffs
10. Coraluppi S (2006) Multistatic sonar localization. *IEEE J Ocean Eng* 31(4):964–974
11. Coraluppi S, Carthel C (2004) Multi-hypothesis sonar tracking. In: Proceedings of the 7th international conference on information fusion. International Society of Information Fusion, Stockholm, Sweden
12. Coraluppi S, Carthel C (2005) Distributed tracking in multistatic sonar. *IEEE Trans Aerosp Electron Syst* 41(3):1138–1147
13. Department of the Navy-United States of America (2004) The Navy unmanned undersea vehicle (UUV) master plan
14. Eickstedt D, Benjamin M (2006) Cooperative target tracking in a distributed autonomous sensor network. In: Proceedings of the IEEE/MTS oceans 2006 conference, Boston, MA, USA
15. Eickstedt D, Benjamin M, Schmidt H, Leonard J (2006) Adaptive control of heterogeneous marine sensor platforms in an autonomous sensor network. In: Proceedings of the IEEE/RSJ international conference on intelligent robots and systems, Beijing, China
16. Eickstedt DP, Schmidt H (2003) A low-frequency sonar for sensor-adaptive, multi-static, detection and classification of underwater targets with AUVs. In: Proceedings of the IEEE/MTS oceans 2003 conference, San Diego, CA, USA
17. Eustice RM (2005) Large-area visually augmented navigation for autonomous underwater vehicles. Ph.D. thesis, Massachusetts Institute of Technology and Woods Hole Oceanographic Institution, Cambridge, MA, USA
18. Fallon M, Papadopoulos G, Leonard J, Patrikalakis N (2010) Cooperative AUV navigation using a single maneuvering surface craft. *The International Journal of Robotics Research*, pp 1461–1474
19. Freitag L, Grund M, Singh S, Partan J, Koski P, Ball K (2005) The WHOI micro-modem an acoustic communications and navigation system for multiple platforms. In: Proceedings of the IEEE/OES oceans 2005 conference, Washington, DC
20. Gadre A, Maczka D, Spinello D, McCarter B, Stilwell D, Neu W, Roan M, Hennage J (2008) Cooperative localization of an acoustic target using a team of AUVs. In: Proceedings of the IEEE/OES autonomous underwater vehicles conference, Woods Hole, MA, USA, pp 64–71
21. Hamilton MJ, Kemna S, Hughes D (2010) Antisubmarine warfare applications for autonomous underwater vehicles: the GLINT09 sea trial results. *J Field Robot* 27(6):890–902 (Special Issue: State of the Art in Maritime Autonomous Surface and Underwater Vehicles, Part 1)
22. Hughes DT, Been R, Vermeij A (2008) Heterogeneous underwater networks for ASW: technology and techniques. In: *Maritime systems and technology*, Genova, Italy
23. Hutchins R, Roque J (1995) Filtering and control of an autonomous underwater vehicle for both target intercept and docking. In: Proceedings of the 4th IEEE conference on control applications. IEEE, pp 1162–1163
24. Jane's IHS (2011) Jane's unmanned maritime vehicles and systems. <http://jumv.janes.com>. Accessed 5 June
25. Johnson-Roberson M, Pizarro O, Williams SB, Mahon I (2010) Generation and visualization of large-scale three-dimensional reconstructions from underwater robotic surveys. *J Field Robot* 27(1):21–51
26. Knight WC, Pridham RG, Kay SM (1981) Digital signal processing for sonar. *Proc IEEE* 69(11):1451–1506
27. Kruger D, Stolkin R, Blum A, Briganti J (2007) Optimal AUV path planning for extended missions in complex, fast-flowing estuarine environments. In: IEEE international conference on robotics and automation (ICRA), Rome, Italy, pp 4265–4270
28. Laterveer R (2003) Abel multistatic sonar information processing chain. Tech. Rep. Technical Memo RL-JUN03-01, NURC, La Spezia, Italy. NATO UNCLASSIFIED
29. LePage KD (2010) An SNR maximization behavior for autonomous AUV control. In: Proceedings of the 10th European conference on underwater acoustics—ECUA 2010, Istanbul, Turkey
30. Lum R, Balasuriya A, Schmidt H (2009) Multistatic processing and tracking of underwater target using autonomous underwater vehicles. In: Proceedings of the 3rd underwater acoustics measurement conference, Nafplion, Greece. <http://www.uam2009.gr>. Accessed 11 Dec 2009
31. Maczka D, Spinello D, Stilwell DJ, Gadre AS, Neu WL (2009) Coordinated tracking of an acoustic signal by a team of autonomous underwater vehicles. In: AUVSI's unmanned systems North America, Washington, DC, USA
32. Maguer A, Dymond R, Mazzi M, Biagini S, Fioravanti S (2008) SLITA: a new slim towed array for AUV applications. In: *Acoustics08*, Paris, France, pp 141–146
33. Newman PM, Leonard JJ, Rikoski RJ (2003) Towards constant-time SLAM on an autonomous underwater vehicle using synthetic aperture sonar. In: Proceedings of the eleventh international symposium on robotics research, Sienna, Italy
34. Pêtrès C, Pailhas Y, Patrón P, Petillot Y, Evans J, Lane D (2007) Path planning for autonomous underwater vehicles. *IEEE Trans Robot* 23(2):331–341
35. Pfeifer R, Scheier C (2001) *Understanding intelligence*. MIT Press, Cambridge
36. Poulsen A, Eickstedt D, Ianniello J (2006) Bearing stabilization and tracking for an AUV with an acoustic line array. In: Proceedings of the IEEE/MTS oceans 2006 conference, Boston, MA, USA
37. Sindt JC, de Theije PAM (2003) Target localisation with multistatic systems. In: Proceedings of the 7th European conference on underwater acoustics—ECUA 2004, Delft, The Netherlands
38. Urick RJ (1983) *Principles of underwater sound*, 3rd edn. McGraw-Hill, New York
39. Williams D (2010) On optimal AUV track-spacing for underwater mine detection. In: Proceedings of the IEEE international conference on robotics and automation (ICRA), Anchorage, AK, USA
40. Williams SB, Pizarro O, Webster JM, Beaman RJ, Mahon I, Johnson-Roberson M, Bridge TCL (2010) Autonomous underwater vehicle-assisted surveying of drowned reefs on the shelf edge of the great barrier reef, australia. *J Field Robot* 27(5):675–697
41. Yao Y, Xu D, Yan W, Li H (2009) An optimal measure choosing strategy to AUVs cooperative localization. In: 4th IEEE conference on industrial electronics and applications (ICIEA), Xi'an, China, pp 1889–1894
42. Zhang L, Liu M, Xu D, Yan W (2009) Cooperative localization for underwater vehicles. In: 4th IEEE conference on industrial electronics and applications (ICIEA), Xi'an, China, pp 2524–2527

Document Data Sheet

<i>Security Classification</i>		<i>Project No.</i>
<i>Document Serial No.</i> NURC-PR-2012-008	<i>Date of Issue</i> April 2012	<i>Total Pages</i> 14 pp.
<i>Author(s)</i> Kemna, S., Hamilton, M.J., Hughes, D.T., LePage, K.D.		
<i>Title</i> Adaptive autonomous underwater vehicles for littoral surveillance. The GLINT10 field trial results.		
<i>Abstract</i> <p>Autonomous underwater vehicles (AUVs) have gained more interest in recent years for military as well as civilian applications. One potential application of AUVs is for the purpose of undersea surveillance. As research into undersea surveillance using AUVs progresses, issues arise as to how an AUV acquires, acts on, and shares information about the undersea battle space. These issues naturally touch on aspects of vehicle autonomy and underwater communications, and need to be resolved through a spiral development process that includes at sea experimentation. This paper presents a recent AUV implementation for active antisubmarine warfare tested at sea in the summer of 2010. On-board signal processing capabilities and an adaptive behavior are discussed in both a simulation and experimental context. The implications for underwater surveillance using AUVs are discussed.</p>		
<i>Keywords</i> Autonomous underwater vehicle – Autonomy - Behavior-based robotics - Target localization and tracking - On-board processing - Multi-static active sonar		
<i>Issuing Organization</i> NURC Viale San Bartolomeo 400, 19126 La Spezia, Italy [From N. America: NURC (New York) APO AE 09613-5000]		Tel: +39 0187 527 361 Fax:+39 0187 527 700 E-mail: library@nurc.nato.int